Neural Computing and Applications (2019) 31:4137–4155
https://doi.org/10.1007/s00521-017-3309-9

ORIGINAL ARTICLE

Efficient control of integrated power system using self-tuned fractional-order fuzzy PID controller

K. Nithilasaravanan[1] · Nitisha Thakwani[1] · Puneet Mishra[2] · Vineet Kumar[1] · K. P. S. Rana[1]

Received: 8 December 2016 / Accepted: 27 December 2017 / Published online: 15 January 2018

Abstract
The integrated power system (IPS) uses various autonomous generation and energy storage systems like aqua electrolyzer, battery, diesel engine, flywheel, fuel cell, solar photovoltaic, ultracapacitor, wind turbine, etc. These may be switched on/off and may run at higher/lower power outputs, at different times. Additionally, IPS is also subjected to parameter variations of its components and the load. As a result, the frequency of an IPS fluctuates from the nominal desired value and therefore it requires a robust controller to accomplish the above-mentioned task. In this work, a self-tuned fractional-order fuzzy PID (STFOFPID) controller, tuned using cuckoo search algorithm, is investigated for efficient control of IPS. STFOFPID is essentially a Takagi–Sugeno model-based fuzzy adaptive controller comprising of non-integer-order differ-integral operators. To assess the relative performance of STFOFPID controller, it is compared with its integer-order counterpart on the basis of their respective objective function value defined as the sum of integral of squared error and integral of squared deviation of controller output. Intensive LabVIEW-based simulation studies have indicated the robustness and hence superiority of STFOFPID controller over its integral counterpart.

Keywords Self-tuned fractional-order fuzzy PID controller · Integrated power system · Renewable energy generation · Efficient control · Robust control · Cuckoo search algorithm

1 Introduction

Diminishing conventional sources of energy such as fossil fuel has made people interested in renewable alternatives. There are many types of renewable sources, and each of them has their own merits and demerits. Using only one for a specific application may not be sufficient as these are nature dependent and are prone to oscillations. To cater to the needs of constant and continuous quality power supply, the concept of hybrid micro-grids has evolved, which has become indispensible for all future needs. Hvelplund has emphasized the need for established local markets in order to secure the technical integration of a large proportion of wind power and other renewable energy sources into the hybrid micro-grids [1]. Integrated power system (IPS) [2] uses various autonomous power generation systems, like aqua electrolyzer (AE), battery energy storage system (BESS), diesel engine generator (DEG), flywheel energy storage system (FESS), fuel cell (FC), solar photovoltaic (PV), ultracapacitor (UC), etc. Apart from reducing carbon emission, these micro-grids are also credited with the

✉ Vineet Kumar
vineetkumar27@gmail.com
http://www.nsit.ac.in

K. Nithilasaravanan
nithu.95@gmail.com
http://www.nsit.ac.in

Nitisha Thakwani
nitishathakwani@gmail.com
http://www.nsit.ac.in

Puneet Mishra
puneet.mishra@ymail.com
http://www.gla.ac.in

K. P. S. Rana
kpsrana1@gmail.com;
http://www.nsit.ac.in

[1] Division of Instrumentation and Control Engineering, Netaji Subhas Institute of Technology, Azad Hind Fauj Marg, Dwarka, New Delhi 110078, India

[2] Department of Electronics and Communication Engineering, GLA University, Mathura, U.P. 281406, India

unique features such as decentralization, autonomous, higher grid resilience while helping in mitigating grid disturbances [3, 4]. Further, to compensate the failure of any component in the micro-grid, alternative energy storage devices like battery, ultracapacitor and flywheel [5] have also been employed. To effectively manage the micro-grid, a control scheme is usually employed whose task is to effectively balance the demand and supply by minimizing the fluctuations in load frequency [6, 7].

2 Literature survey

To minimize the deviation in frequency, integration of different energy resources like offshore wind, PV, FC and DEG along with the energy storage elements like FESS and BESS has been reported by [8]. This work uses UC as an alternative energy storage element, and proportional–integral (PI) controller is employed to achieve further improvements in the deviation of frequency profiles. Simplicity, ease in designing, robustness, wide range of applicability and near-optimal performance are some of the key reasons that have made PID controller popular in the academic and industry sectors [9–13]. However, with the application of PID controller, it is generally difficult to achieve the desired control performance in the presence of unknown nonlinearities, time delays and model uncertainties. To overcome these limitations, intelligent control schemes such as fuzzy logic have been employed for effective control of complex plants [14, 15].

The basic idea behind fuzzy logic technique has been to incorporate a model that could emulate the experience of a human process operator in design of controller. Fuzzy logic, on the concept of fuzzy sets, was first proposed by Prof. Zadeh [16]. This work was further expanded by the introduction of linguistic variables, which equate to a variable defined as a fuzzy set [17–19]. One of the most famous applications of fuzzy logic is control engineering, and it has attracted scientists as well as industrial researchers. Mamdani and Assilian presented the first successful attempt of fuzzy logic to efficiently control a laboratory scale plant [20–23]. Further, Holmblad and Ostergaard [24] presented the first industrial application of fuzzy controllers to control cement kilns. Fuzzy logic has also been applied to linguistic controller rules, which reduces the controller to a conventional nonlinear controller, allowing the usage of nonlinear control theory techniques [25]. Various types of fuzzy logic controllers were presented in numerous works, such as [26−28], self-tuning fuzzy controller [29], stable adaptive fuzzy controller [30], single-input fuzzy logic controller [31], amongst many others. Also, some of the interesting applications of soft computing techniques are reported in [32–37]. To summarize, a detailed survey of fuzzy control was presented in [15, 38].

Recently, fractional calculus-based control systems have been claimed to be more robust over their integer-order counterparts. Therefore, these have gained popularity, particularly in the fields of control engineering such as process control, nuclear reactor control, robotics, chaos synchronization. Fractional calculus when incorporated with fuzzy logic has shown superior results. Recent developments in this field are more amenable to the use of controllers that are intelligent, adaptive, nonlinear, or a combination of these such as fuzzy logic control, nonlinear model predictive control, etc. A fractional-order fuzzy PID (FOFPID) controller has been successfully applied to two-link robotic manipulator, and it has demonstrated superior results over its integer counterpart [39]. Further, a robust fractional-order fuzzy P + fuzzy I + fuzzy D has also been used for the control of a two-link planar rigid manipulator and it has been compared with its integer-order counterpart, and results demonstrated that fractional-order controller was more robust as it provides additional degrees of freedom [40]. More recently, fractional-order fuzzy PD (FOFPD) and fractional-order fuzzy PI (FOFPI) nonlinear controllers were used as primary and secondary controllers, for the speed control of hybrid electric vehicle [41]. The work concluded that the combination of FOFPD and FOFPI controllers outperformed rest of the controllers under study and thus is more robust. Several works have been reported in the literature, which successfully demonstrate the robustness feature of the FOPID controller [42, 43].

The existence of stochastic renewable energy generation systems in the IPS, like solar power and wind, leads to continuous variations in grid frequency, which affects the quality of power. Nominally, the fluctuations in the grid frequency should be kept within the prescribed limit in order to safely operate all the electrical loads connected to it. For this purpose, a control mechanism is required which sends a control signal to the energy-storing devices, i.e. to absorb excess power from the grid and to release deficit power back into the grid, according to the supply and demand requirements. Also, it is expected from the control scheme that DEG should discharge high bursts of power back into the grid in order to meet short-term demands of the load. To accomplish this control objective, researchers have traditionally used an independent controller for each of the attached components and hence, several controllers were required to effectively control the IPS as reported in [8, 44]. Each of these controllers has multiple parameters, and therefore, their tuning and implementation becomes a tedious task. In the light of above-mentioned facts, an

efficient, centralized, adaptive and a stand-alone control scheme becomes pivotal in the working of an IPS.

To cater to the above-mentioned requirements, in this paper, a robust, adaptive, centralized, stand-alone controller, namely self-tuned fractional-order fuzzy PID (STFOFPID) controller has been proposed. It is essentially a Takagi–Sugeno (TS)-based adaptive fuzzy controller having non-integer-order differ-integral operators. Its performance has been compared with self-tuned integer-order fuzzy PID (STIOFPID) controller, on the basis of an objective function defined as the sum of integral of squared error (ISE) and integral of squared deviation of controller output (ISDCO). The parameters of both the controllers were optimized with the help of the cuckoo search algorithm (CSA). The controllers were then tested for robustness by varying the parameters of UC, disconnecting certain generation and storage blocks, and adding a rate constraint-type nonlinearity in the feedback path. All the above-mentioned tests helped in comparing the two controllers and established their relative usefulness in controlling the IPS. The main contributions of this paper are as follows:

(1) A centralized and adaptive control scheme, namely STFOFPID has been presented for the efficient control of the IPS.
(2) STFOFPID adjusted its parameters at runtime, depending upon the error and rate of change of error.
(3) STFOFPID controller, being self-tuned, is found to be robust as it could withstand fluctuations with relative ease and produced a constant output.

Further, rest of the paper has been organized as follows. Following a brief introduction in Sects. 1 and 2 provides a literature survey of the established techniques for IPS control and application of fractional-order calculus in control applications. All the mathematical details including the equations, transfer functions, parameter values of the various energy-storing/generating components have been described in this Sect. 3. Section 4 presents the details of the used controllers, i.e. STIOFPID and STFOFPID. This is followed by a brief introduction to the optimizing technique, CSA used to optimize the parameters of the fuzzy controllers. Section 5 presents simulation results and analysis of the conducted tests such as disconnecting various components from IPS, variation in the system parameters to test controllers' robustness. Statistical analysis of the performance of considered controllers is also presented in this section. Section 6 summarizes and concludes the paper.

3 Plant description and problem formulation

The schematic of IPS that has been used in this work is shown in Fig. 1 along with the corresponding block diagram representation as depicted in Fig. 2. As seen in Figs. 1 and 2, the used IPS includes various modes of energy generation as well as storage. Each of the used components is described with the help of a transfer function. Components AE, DEG, FC, STPG and WTG are modelled by first-order dynamics with the help of their gains and time constants, given in Table 1 [45]. Section 3.1 presents the mathematical equations of the generation components of the IPS. Section 3.2 presents the same for the storage components followed by the model of the power system in Sect. 3.3. Section 3.4 presents the stochastic model of renewable energy blocks and the demand load. Section 3.5 formulates the problem that has been addressed in this paper.

3.1 Mathematical models of generation systems used

This subsection describes the mathematical models of various components used in the IPS. The control action implemented by the employed controller in the following models is represented by Δu.

Diesel Engine Generator A DEG consists of a diesel engine, a generator and various ancillary devices (control systems, circuit breakers, starters). Equation (1) represents the DEG model

$$G_{\mathrm{DEG}}(s) = \frac{K_{\mathrm{DEG}}}{1 + sT_{\mathrm{DEG}}} = \frac{\Delta P_{\mathrm{DEG}}}{\Delta u}, \tag{1}$$

where, K_{DEG}: gain of DEG, T_{DEG}: time constant of DEG.ΔP_{DEG}: power output from DEG.

Fuel Cell FC is a device that generates electricity by a chemical reaction. It has two electrodes, positive and negative, known as the anode and cathode, respectively. Multiple FCs are used in a stack so as to supply a considerable amount of electricity. FC model is described by Eq. (2).

$$G_{\mathrm{FC}_k}(s) = \frac{K_{\mathrm{FC}}}{1 + sT_{\mathrm{FC}}} = \frac{\Delta P_{\mathrm{FC}_k}}{\Delta P_{\mathrm{AE}}},\ k = 1, 2, \tag{2}$$

where, K_{FC}: gain of FC, T_{FC}: time constant of FC, ΔP_{FC_k} Power output from FC, ΔP_{AE} Power output from AE.

Solar Thermal Power Generator STPG is a generation scheme where the sun's rays are used in the heating of the fluid to high temperatures. The steam thus created is used to power the generator to produce electricity

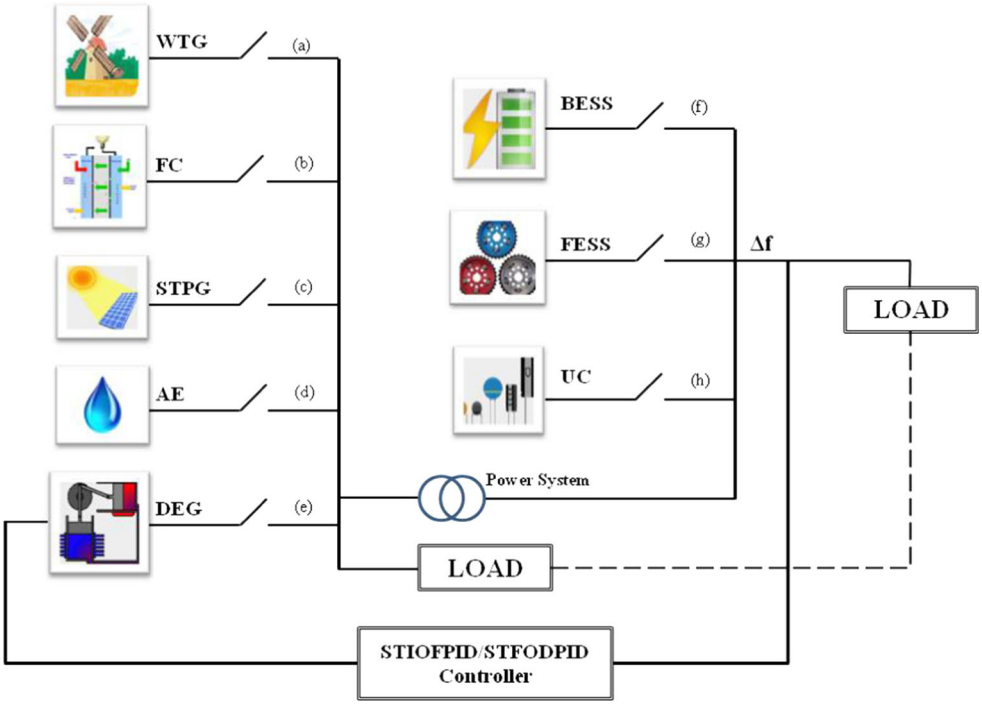

Fig. 1 Schematic diagram of the integrated power system. Here, **a**–**h** are switches that correspond to the disconnection of components due to various reasons

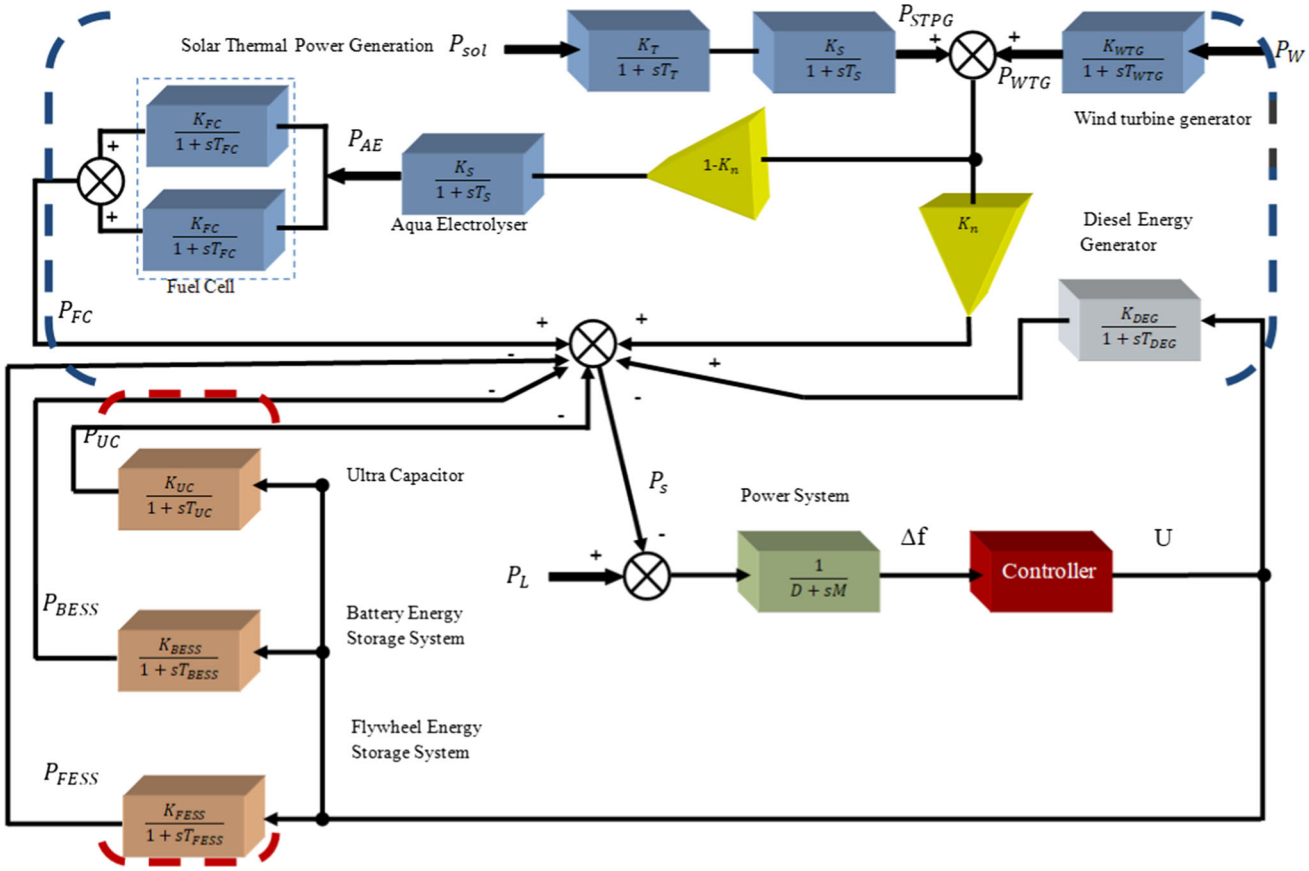

Fig. 2 Block diagram of the plant (integrated power system) with all major components

Table 1 Gain and time constants of various components

Component	Gain (K)	Time constant (T)
Aqua electrolyzer	0.002	0.5
Battery energy storage system	− 0.003	0.1
Diesel engine generator	0.003	2
Flywheel energy storage system	− 0.01	0.1
Fuel cell	0.01	4
Solar thermal power generator	1.8, 1	1.8, 0.3
Ultracapacitor	− 0.7	0.9
Wind turbine generator	1	1.5

$$G_{\mathrm{STPG}}(s) = \frac{K_s}{1+sT_s}.\frac{K_T}{1+sT_T} = \frac{\Delta P_{\mathrm{STPG}}}{\Delta P_{\mathrm{sol}}}, \tag{3}$$

where, K_S gain of solar part of STPG, T_S time constant of solar part of STPG, K_T gain of thermal part of STPG, T_T time constant of thermal part of STPG, ΔP_{STPG} Power output from STPG, ΔP_{sol} Power input to STPG.

Wind Turbine Generator WTG uses the power of the wind to turn the blades, which in turn spins the shaft connected to a generator, thus producing electricity. Equation (4) presents its model

$$G_{\mathrm{WTG}}(s) = \frac{K_{\mathrm{WTG}}}{1+sT_{\mathrm{WTG}}} = \frac{\Delta P_{\mathrm{WTG}}}{\Delta P_{\mathrm{W}}}, \tag{4}$$

where, K_{WTG} gain of WTG, T_{WTG} time constant of WTG, ΔP_{WTG} power output from WTG, ΔP_{W} power input to WTG.

Aqua Electrolyzer AE is used to convert a part of generated power from renewable energy sources into hydrogen, for the fuel cell. For small signal analysis, the transfer function of AE uses $(1-K_n)$ of the power of STPG and WTG in order to produce H_2, to be used by FCs to produce power and feed it back to the grid.

$$G_{\mathrm{AE}}(s) = \frac{K_{\mathrm{AE}}}{1+sT_{\mathrm{AE}}} = \frac{\Delta P_{\mathrm{AE}}}{(\Delta P_{\mathrm{WTG}} + \Delta P_{\mathrm{STPG}}).(1-K_n)}, \tag{5}$$

where, K_{AE} gain of AE, T_{AE} time constant of AE, ΔP_{AE} power output from AE, ΔP_{WTG} power output from WTG, ΔP_{STPG} power output from STPG.

$$K_n = P_t/(P_{\mathrm{WTG}} + P_{\mathrm{STPG}}) \tag{6}$$

$$K_n = 0.6$$

3.2 Mathematical models of energy storage systems

In IPS of Fig. 2, FESS, BESS and UC are connected and are driven by the output signal from the controller. These components are connected in the feedback loop, and they absorb or release energy from or to the grid. Their transfer functions are given as follows. The control action implemented by the employed controller in the following models is represented by Δu.

Flywheel Flywheel store kinetic energy by continuously spinning a compact rotor in a low-friction environment. The kinetic energy stored is directly proportional to the mass of the rotor, the square of the radius and the square of the rotational speed.

$$G_{\mathrm{FESS}}(s) = \frac{K_{\mathrm{FESS}}}{1+sT_{\mathrm{FESS}}} = \frac{\Delta P_{\mathrm{FESS}}}{\Delta u}, \tag{7}$$

where, K_{FESS}: gain of FESS, T_{FESS}: time constant of FESS, ΔP_{FESS}: Power output from FESS.

Battery Batteries convert electricity into chemical potential energy for storage and back into electrical energy as needed. BESS comprises of batteries, control and power conditioning system (C-PCS) and rest of the plant, which provides good protection for batteries and C-PCS.

$$G_{\mathrm{BESS}}(s) = \frac{K_{\mathrm{BESS}}}{1+sT_{\mathrm{BESS}}} = \frac{\Delta P_{\mathrm{BESS}}}{\Delta u}, \tag{8}$$

where, K_{BESS}: gain of BESS, T_{BESS}: time constant of BESS, ΔP_{BESS}: Power output from BESS.

Ultracapacitor UC stores energy by physically separating negative and positive charges. The charges are stored on two parallel plates, which are divided by an insulating material. UCs have a fairly long cycle life as there are no chemical variations on the electrodes of the UC.

$$G_{\mathrm{UC}}(s) = \frac{K_{\mathrm{UC}}}{1+sT_{\mathrm{UC}}} = \frac{\Delta P_{\mathrm{UC}}}{\Delta u}, \tag{9}$$

where, K_{UC} gain of UC, T_{UC} time constant of UC, ΔP_{UC} Power output by UC.

3.3 Mathematical model of power system using deviation in grid frequency

The power system in the IPS is modelled using the DEG. The transfer function of the power system is given by

$$G_{\mathrm{sys}}(s) = \frac{\Delta f}{\Delta P_e} = \frac{1}{D+M_s}, \tag{10}$$

where, M_s: equivalent inertia constant (taken as 0.4 for this study), D equivalent damping constant (taken as 0.03 for this study)

3.4 Stochastic model of the renewable energy components and load

The solar, wind generation and load demand are modelled taking into account all nonlinearities including deterministic drift and stochastic variations (Fig. 3). The models

engender an average value and stochastic variation about the average generated/demand power at each time instant [44]. A greater variation in the parameters is reflected by a sudden shift in the average value at a particular time instant. The template used for this model is as follows:

$$P = ((\Phi\eta\sqrt{\beta}(1 - G(s)) + \beta)\delta/\beta)\Gamma = \xi \cdot \Gamma, \tag{11}$$

where, P output power of the wind, solar and the load model, Φ Power's stochastic component, β contributor to average power value, G(s) low pass transfer function, ξ generated or demand power η, δ : normalizing constants, used in normalizing generated/demand powers to match the (p.u.) level Γ: time-dependent switching signal; directs the sudden variation in average value for the output

The parameters used for generation of wind power (P_{WTG}) are:

$$\begin{aligned} \Phi &\sim U(-1,1),\ \eta = 0.8, \beta = 10 \\ G(s) &= 1/(10^4 s + 1), \delta = 1 \\ \Gamma &= 0.5H(t) - 0.1H(t-40) \end{aligned} \tag{12}$$

The parameters used for generation of solar power (P_{STPG}) are:

$$\left.\begin{aligned} \Phi \sim U(-1,1),\ \eta = 0.7, \beta = 2 \\ G(s) = 1/(10^4 s + 1), \delta = 0.1 \\ \Gamma = 1.1111H(t) - 0.5555H(t-40) \end{aligned}\right\} \tag{13}$$

The parameters used of the demand load (P_{L}) are:

$$\left.\begin{aligned} \Phi \sim U(-1,1),\ \eta = 0.8, \beta = 100, \\ G(s) = (300/(300s+1)) - (1/(1800s+1)), \delta = 1 \\ \Gamma = H(t) + (0.8/\xi)H(t-80) \end{aligned}\right\} \tag{14}$$

where, H (t) is the Heaviside step function.

Figure 3 shows a single realization of the stochastic blocks, generated powers (P_{W}, P_{sol}), demand (P_{L}) and the net generated power (P_t). From Fig. 3, it can be seen that for all the cases, there is a random component superimposed over a nominal value and there are jumps from the nominal value at random instants of time, which shows a sudden change in the level of the power at different times. Here, the change occurs at about 40 s for P_{WTG}, P_{STPG} and P_t and 80 s for P_{L}. Also, all the powers are considered in watt.

3.5 Problem formulation

The controllers used in the past faced the challenge of providing stable power. Added to this, the controllers were also not immune enough to variations in parameters of various power generating and storage elements. This led to their poor robustness and reliability as continuous changes in grid frequency affects the power quality [46, 47]. To overcome this, the fluctuation in the grid frequency should be kept in specified bounds. To achieve this complex task, an efficient control mechanism is required, which transmits a control signal to the energy-storing devices, i.e. to absorb the additional power from the grid and to release the deficit power back into the grid accordingly. Further, the control scheme must also be able to accommodate the diesel engine's high burst discharge of power into the grid in order to meet short-term demands of the load. Furthermore, a controller must be able to handle the uncertainty of the renewable sources, both the variations and the complete disconnection of the source itself, from the system. It is worth mentioning that, in the past, a separate controller was used in each loop. This strategy of using a separate controller in each loop in the IPS leads to complexity and difficulty in the tuning of the controllers. This very fact has evolved the concept of a centralized controller. This

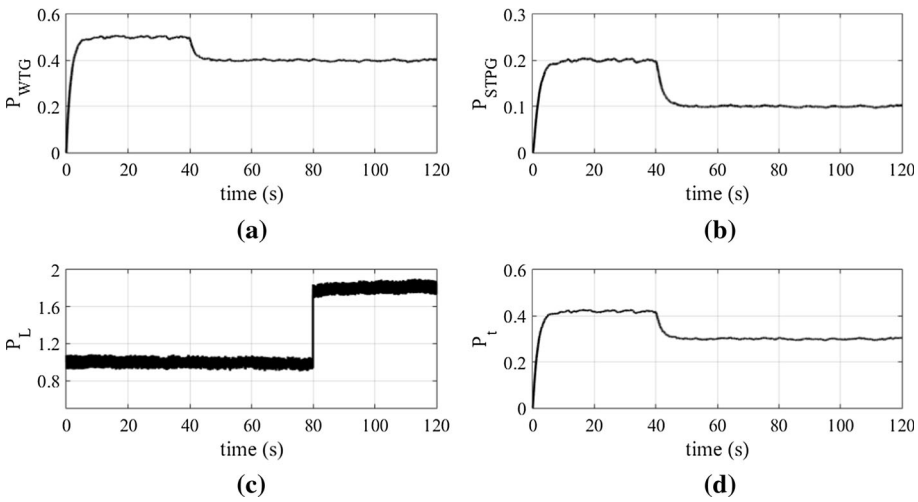

Fig. 3 Renewable power generation and load (single iteration) plots **a** WTG, **b** STPG, **c** load, **d** total

centralized controller is expected to be a stand-alone solution having all the above-mentioned features. Furthermore, the adaptive centralized controller would be an added advantage for the IPS as it will be able to offer efficient run time corrections while being a stand-alone solution. This paper is motivated to explore the application of STFOFPID as an adaptive stand-alone solution for IPS. Later, it will be shown that STFOFPID is a robust, variation resistant and centralized controller to effectively control the IPS.

4 Structure of fuzzy controllers

The two investigated controllers in this work are STIOFPID and STFOFPID. The basic architecture of these controllers consists of the combination of self-tuned fuzzy PI and fuzzy PD controllers, i.e. $FPI + FPD$ controller. Brief designs of both the controllers have been described in the following subsections.

4.1 STIOFPID controller

The STIOFPID controller [48], shown in Fig. 4, is essentially a formula-based fuzzy controller (FBFC) [49]. This controller is a variable gain TS fuzzy controller, which was developed in 1985 and is a ubiquitous controller. Error (e) and rate of change of error (r) are the two linguistic variables in this controller, which are expressed using two membership functions, namely positive (P) and negative (N). For added precision, scaling factors have been added to the 'e' and 'r' signals. K_e and K_p are the scaling factors added to the 'e' and 'r' signals, respectively.

The two membership functions, shown in Fig. 5, are characterized by 'L', which is a real number. These functions are symmetrical in the universe of discourse.

The rule base of the FBFC has rules of the form,

$$\left.\begin{aligned} e' = K_e.e \text{ and } r' = K_r.r \\ R_i : \text{IF } \text{`}e'\text{'} \text{ is } P_j \text{ and } \text{`}r'\text{'} \text{ is } P_k \text{ then } q_i = a_i e' + b_i r' \\ \text{where } i = 1,2,3,4, j = 1,2 \text{ and } k = 1,2 \end{aligned}\right\} \tag{15}$$

$R_i = i$th rule of the FBFC controller, $P_j =$ membership function defined for e', $P_k =$ membership function defined for r', $q_i =$ next part of the ith rule, a_i, $b_i =$ real constants.

The output of FBFC is computed through the instantaneous value of the error, '$e'(t)$' and the rate of change of error, '$r'(t)$'. Here, the entire two-dimensional space created by inputs to the controller (e'(t) and r'(t)) is distributed into 20 input combination (IC) regions. These IC regions are based upon the membership functions. Thus, any point in the $e'(t)$ $r'(t)$ plane would lie in any one of the 20 IC regions, and each IC region has a formula assigned to it. These formulae essentially determine the output of the controller as described in [49]. This output of the controller is further used to get the final outputs for both the controllers.

The STIOFPID controller consists of two components, i.e. fuzzy PI (velocity form) and fuzzy PD (position form) controllers. Conventionally, the velocity form of a PI controller in linear form is given by:

$$\Delta u_{PI}(nT) = K_i e'(nT) + K_p r'(nT) \tag{16}$$

And the linear form of PD controller in position form is given by:

$$u_{PD}(nT) = K_i e'(nT) + K_p r'(nT) \tag{17}$$

Further, the output of the controller is evaluated as,

$$\left.\begin{aligned} \Delta u_{\text{FPI}}(\text{or } u_{\text{FPD}}) = \frac{\sum_{i=1}^{4} \Delta u_i \mu_{R_i}}{\sum_{i=1}^{4} \mu_{R_i}} \\ \Delta u_{\text{FPI}}(\text{or } u_{\text{FPD}}) = \sum_{i=1}^{4} \frac{\mu_{R_i}}{\sum_{i=1}^{4} \mu_{R_i}} (a_i e'(nT) + b_i r'(nT)) \end{aligned}\right\} \tag{18}$$

$$\left.\begin{aligned} \Delta u_{\text{FPI}}(\text{or } u_{\text{FPD}}) = \sum_{i=1}^{4} \left(K_1^i(e', r') e'(nT) + K_2^i(e', r') r'(nT)\right) \\ \Delta u_{\text{FPI}}(\text{or } u_{\text{FPD}}) = K_1 e'(nT) + K_2 r'(nT) \end{aligned}\right\} \tag{19}$$

$$K_1^i = \frac{\mu_{R_i} a_i}{\sum_{i=1}^{4} \mu_{R_i}} \text{ and} \tag{20}$$

$$K_2^i = \frac{\mu_{R_i} b_i}{\sum_{i=1}^{4} \mu_{R_i}}, \; i = 1,2,3,4. \tag{21}$$

The adaptability of the FBFC gains comes from the fact that these gains vary in run time according to the rule base of FBFC. The values of the nonlinear gains, K_1 and K_2 can be written as

$$K_1(e'(nT), r'(nT)) = \sum_{i=1}^{4} K_1^i(e'(nT), r'(nT)) \tag{22}$$

and

$$K_2(e'(nT), r'(nT)) = \sum_{i=1}^{4} K_2^i(e'(nT), r'(nT)) \tag{23}$$

The output of the FPID controller is the summation of two components, i.e. fuzzy PI and PD. This can be written as

$$u_{\text{STIOFPID}} = K_{\text{PI}} \int (\Delta u_{\text{STIOFPI}}) \mathrm{d}t + K_{\text{PD}} u_{\text{STIOFPD}}, \tag{24}$$

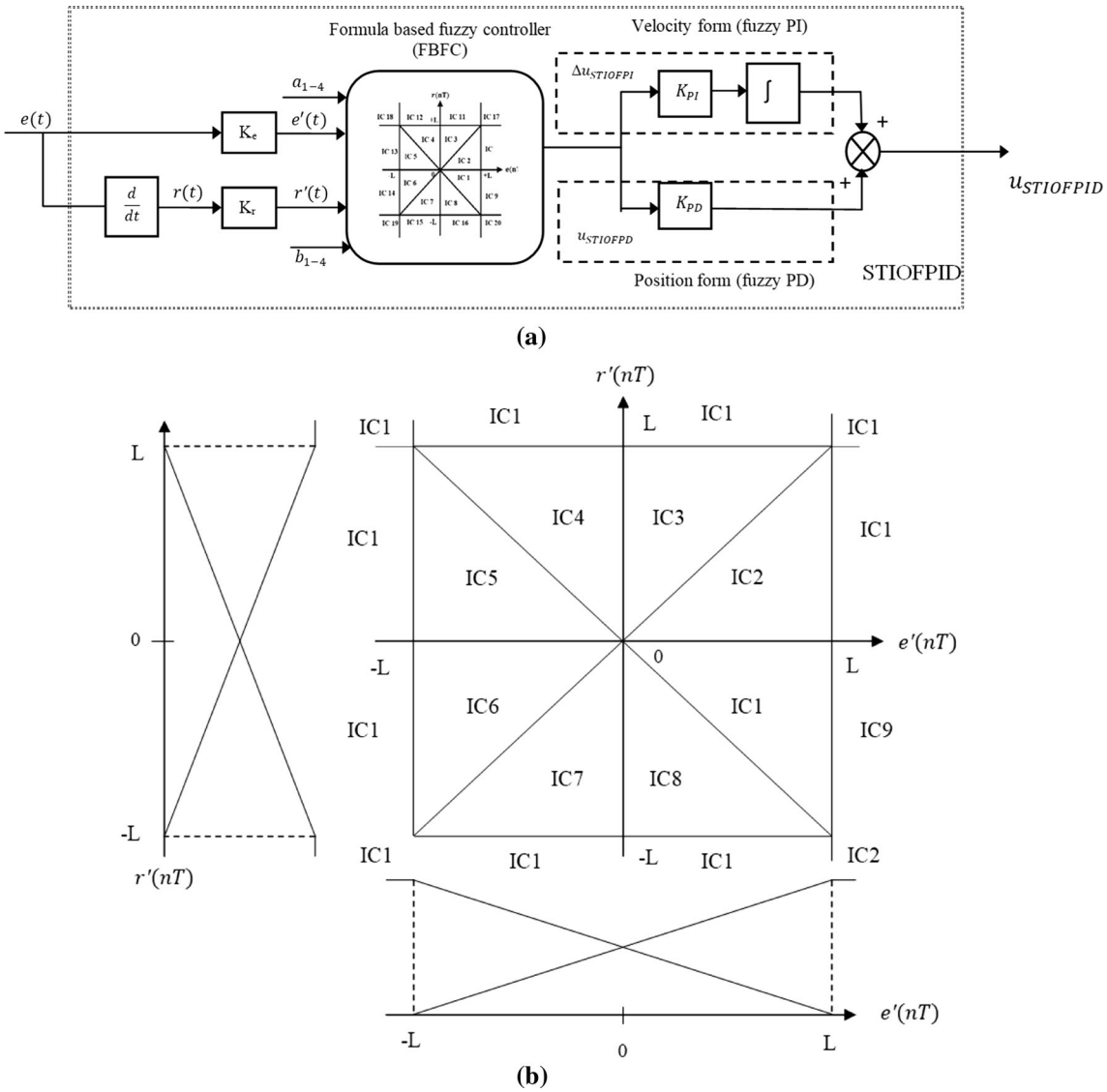

Fig. 4 **a** Structure of STIOFPID controller, **b** division of input space for deriving structure of the fuzzy PI and fuzzy PD components of STIOFPID controller

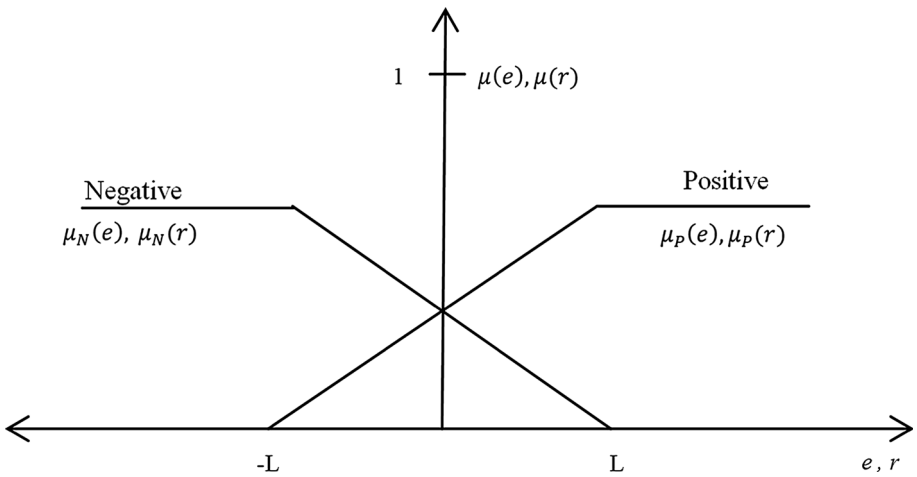

Fig. 5 Variation of '***e***' and '***r***' in the membership function

where, u_{STIOFPID} output of STIOFPID controller, u_{STIOFPI} fuzzy PI component generated by FBFC, u_{STIOFPD} fuzzy PD component generated by FBFC, K_{PI},K_{PD} scaling factor of fuzzy PI and fuzzy PD components, for an additional degree of flexibility.

From Eq. 24, it may be observed that the FBFC output is taken in two forms, i.e. one in velocity form (which is to be integrated to find the final instantaneous output), and other in position form (which can be directly taken to find the final instantaneous output). This implementation of getting a fuzzy PID action is mostly used in various research studies. The reason for the same is the very complex implementation and behaviour of fuzzy PID controller having three inputs, viz. error, integration of error and derivative of error. For a fuzzy rule base having three inputs and seven membership functions for each input, there will be a total of 343 rules in the rule base of the controller, which is very complex to be implemented. However, the method used in this paper only uses a single block, i.e. FBFC, whose output taken in two different forms, viz. position and velocity form, as shown in Fig. 4a, can directly generate a self-tuning fuzzy PID or rather, $PI + PD$ action. Also, this method of generating a fuzzy PID action creates no additional change in the rule base of FBFC controller, and the structure remains very simple in contrast to a fuzzy controller with three linguistic inputs.

4.2 STFOFPID controller description

The STFOFPID controller is similar to a STIOFPID controller, with one major difference to generate the rate of change of error ($r'(t)$), the latter uses a fractional-order differentiator, and to generate the fuzzy PI action, a fractional-order integrator is used to integrate the output of FBFC. Further, the STIOFPID controller uses the same FBFC structure, but with different values of the parameters for its implementation. Due to this reason, the variations of K_1 and K_2 gains of FBFC (for STFOFPID controller) will have different nature of variations in the error and rate of change of error space. The schematic of the controller is shown in Fig. 6.

The controller output is stated as:

$$u_{\text{STFOFPID}} = K_{\text{PI}}\left(\frac{d^{-\lambda}}{dt^{-\lambda}}(\Delta u_{\text{STFOFPI}})\right) + K_{\text{PD}}u_{\text{STFOFPD}} \quad (25)$$

4.2.1 Implementation of fractional calculus

In this work, 'Oustaloup approximation' is used for the implementation of fractional-order calculus for continuous time domain. This approximation uses a higher order filter ($2\,N + 1$) and fits the approximation within a given frequency range (ω_L, ω_H). The approximation of s^{μ} can be given as [3]

$$s^{\mu} \approx K' \prod_{k=-N}^{k=N} \frac{s + \omega_{Z_k}}{s + \omega_{P_k}} \quad (26)$$

K' gain constant of the analog filter, ω_{Z_k} zeroes of the analog filter given by

$$\omega_{Z_k} = \omega_L$$

ω_{P_k} poles of the analog filter given by

$$\omega_{P_k} = \omega_L\left(\omega_H/\omega_L\right)^{\frac{k+N+\left(\frac{1}{2}\right)(1+\mu)}{2N+1}} \quad (27)$$

N: order of the Oustaloup approximation.

There is a trade-off between ripple reduction and hardware implementation complexity. Higher the value of 'N', lesser will be the ripples in phase response and magnitude of the filter, but will make the hardware implementation more complex. On the other hand, lower the value of 'N', more will be the ripples, however, easier will be the hardware implementation. Thus, a balance has to be maintained between the two parameters and accordingly the value of 'N' is to be decided. In this work, $N = 5$, and $\left[\omega_{L,}\omega_H\right] = [10^{-2}, 10^{2}]$ rad/s.

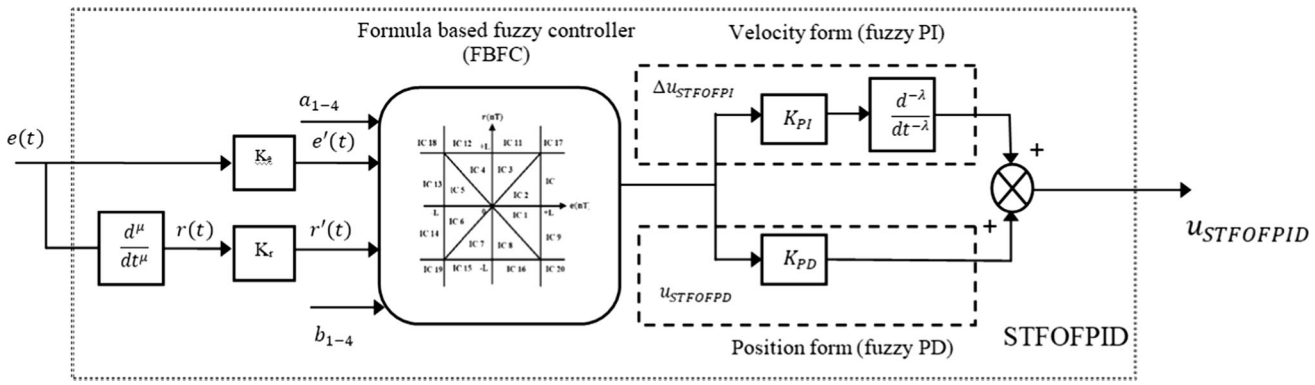

Fig. 6 Structure of STFOFPID controller

4.3 Controller tuning

The parameters of the controllers are tuned with CSA [50–52]. CSA is a relatively new optimization algorithm, developed by [53], and the same has been found to be efficient in solving global optimization problems. It is powerful, nature-inspired metaheuristic algorithm for optimization and computational intelligence. Recent studies show [54, 55] that CSA is potentially far more efficient than its counterparts. This algorithm has the following three idealized rules:

- Each cuckoo lays one egg at a time and dumps it in a randomly chosen nest.
- The best nests with high-quality eggs will be carried over to the next generations.
- The number of available host nests is fixed, and the egg laid by a cuckoo is discovered by the host bird with a probability $\rho_a \in (0, 1)$. In this case, the host bird can either get rid of the egg, or simply abandon the nest and build a completely new nest.

This algorithm uses a balanced combination of a local random walk and the global explorative random walk, controlled by a switching parameter ρ_a.

The local random walk can be written as:

$$x_i^{t+1} = x_i^t + \alpha s \otimes H(\rho_a - \varepsilon) \otimes \left(x_j^t - x_k^t\right), \tag{28}$$

where, x_j^t, x_k^t two different, randomly selected solutions with the aid of random permutation, $H(u)$ Heaviside function, ε random number selected from a uniform distribution, s step size.

On the contrary, global random walk can be given as (as carried out using Lévy flights)

$$x_i^{t+1} = x_i^t + \alpha L(s, \lambda)\{\alpha > 0\} \tag{29}$$

Here, α is the step scaling factor. In most cases, $\alpha = O(L/10)$

$L =$ characteristic scale of the problem of interestand

$$L(s, \lambda) = \frac{\lambda \Gamma(\lambda) \sin\left(\frac{\pi\lambda}{2}\right)}{\pi} \frac{1}{s^{1+\lambda}}, (s \gg s_0 > 0) \tag{30}$$

The above equation is essentially the stochastic equation for a random walk. In the present work, the values of various parameters such as number of nests and rate of discovery of alien eggs have been kept as 20 and 0.25, respectively.

4.4 Optimization of STIOFPID and STFOFPID controller parameters

The objective function (J) for optimization is taken as the weighted sum of squared of frequency deviation and the squared of deviation of control signal u from its nominal steady state values u_{ss}. The objective function J can be defined as:

$$J = \int_0^{T_{max}} (w_1(\Delta f)^2 + w_2(u - u_{ss})^2) \mathrm{d}t \tag{31}$$

The first term in the objective function is the ISE of deviation of grid frequency. The second term of the objective function is the ISDCO. The weights w_1 and w_2 indicate the relative importance of each of the two terms in J. Here, w_1, $w_2 = 1$, to give equal importance to both. The reason for taking this objective function is to take two terms into consideration, one is related to the control performance, i.e. whether the frequency deviation is minimized to zero for overall period of experiment or not. The second term is related to the variation in the controller output. Since larger variation in the controller output may lead to increased rate of wear and tear in the final control elements in the control loop, one should avoid it. The steady state control signal is taken as a reference from where the deviation has to be measured. Evaluating squared deviation from this steady state value ensures that the controller output is not very fluctuating nature and provides a smooth variation in it. Also taking a combined performance index (J = ISE + ISDCO), it has been ensured that mere reducing large fluctuations in the controller output would not interfere with the control performance. Taking ISE into account in calculation of J, it was made sure that controller be tuned in such a way so that there will very less deviation in frequency. It is worth mentioning here that the steady state control signal u_{ss} is taken as,

Table 2 Tuned values of various gains

Gains	STIOFPID	STFOFPID
a_1	5.078	5.270
a_2	3.130	8.710
a_3	6.068	11.703
a_4	21.999	32.130
b_1	6.424	6.249
b_2	0	4.015
b_3	0.456	0
b_4	0.713	1.403
L	1.246	0.073
K_e	0.721	0.437
K_r	0.999	0.975
K_{PI}	0.114	0.193
K_{PD}	0.294	0.248
μ	1	0.822
λ	1	1.009

$$u_{ss} = 0.81H(t) + 0.17H(t-40) + 1.12H(t-80) \quad (32)$$

The tuned gains, obtained by minimizing the fitness function for nominal values of plant parameters as shown in Table 1, are listed in Table 2, for both the controllers.

The presented IPS was modelled in LabVIEW^{TM} environment, and all the simulation results in this work were obtained for a time of 120 s with a fixed step size of 0.01 s using Bogacki–Shampine method of order 3. Figure 7 plots the objective function value versus iterations for both the controllers. Table 2 presents the values of 15 corresponding gains. The gains $a_1 - a_4$, $b_1 - b_4$, L represent the various variables used in the division of input space for analytically deriving structure of the TS fuzzy PI controller.K_e, K_r are the scaling factors for the e (t) and r (t) signals that are input to the controller. K_{PI} and K_{PD} are the scaling factors used to provide an additional degree of freedom in the STFOFPID controller. μ and λ are the derivative and integral fractional orders. Figures 4 and 6 depict the use of these gains.

5 Observations and inferences

The controllers have been tested in multiple conditions so as to prove their respective worth in the IPS. All the tests employed in the following sections simulate real-life conditions. In the following subsections, both the STIOFPID and STFOFPID have been subjected to various tests and conditions in order to evaluate their relative robustness. Results have been organized as follows. Section 5.1 presents the performances of both the controllers under nominal conditions. Section 5.2 presents the performances of the controllers when a nonlinear rate constraint is added to the feedback path in the IPS. Section 5.3 showcases the robustness of the controllers with the variation in UC parameters. Section 5.4 tests the performances of the controllers upon the removal of different energy storage components, whereas Section 5.5 provides a statistical analysis of both the controllers under nominal conditions.

5.1 Controller performance under nominal conditions

For this study, all components are considered to be in linear operation region. As was observed in Fig. 3, both the wind and solar power had variations that are superimposed about the steady state value. Both of these have a sudden drop in the value at 40 s, i.e. both the powers drop to varied levels after 40 s. This simulates the actual real-life scenario where there is vacillation in the power generated, depending on factors such as weather conditions, etc. The power of load also peaks at 80 s, which shows its variations about the steady state values. The objective function values for STIOFPID and STFOFPID controllers under nominal conditions comes out as 3.7756 and 3.69985, respectively.

The Fig. 8 depicts the frequency deviations as well as the control signal curves for both the STIOFPID and the STFOFPID controllers. From the frequency curve, it can be clearly noted that the STFOFPID offered lesser deviation in frequency as compared to its integral counterpart. In Fig. 9, the individual powers of the different components, dependent on the controller output, for both the controllers have been plotted. A very simple thing to note here is that the energy-producing components like FC, DEG have a positive plot while the energy-storing elements like FESS, BESS and UC have a negative plot. It is also noted that UC contributes to the maximum power amongst all the other elements. Figure 9(f) presents the variation in P_S which is the summation of all the powers from all the energy-storing/generating components of the IPS.

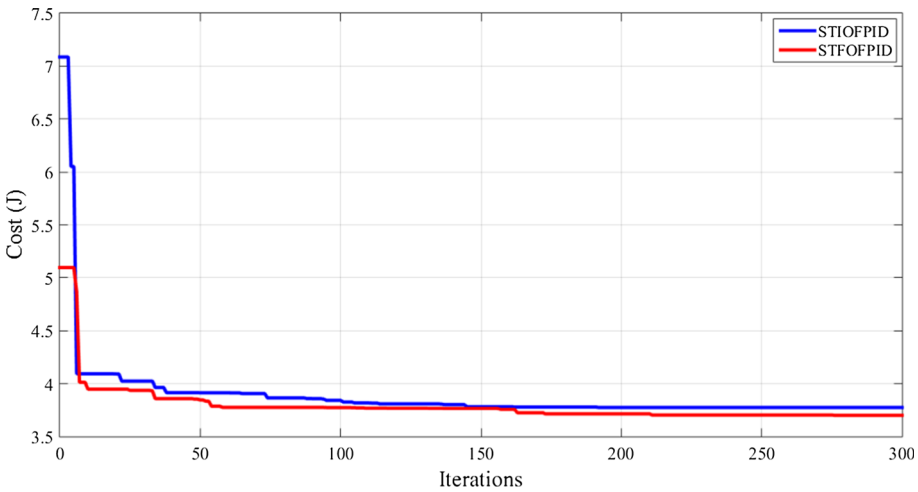

Fig. 7 Convergence curves for CSA

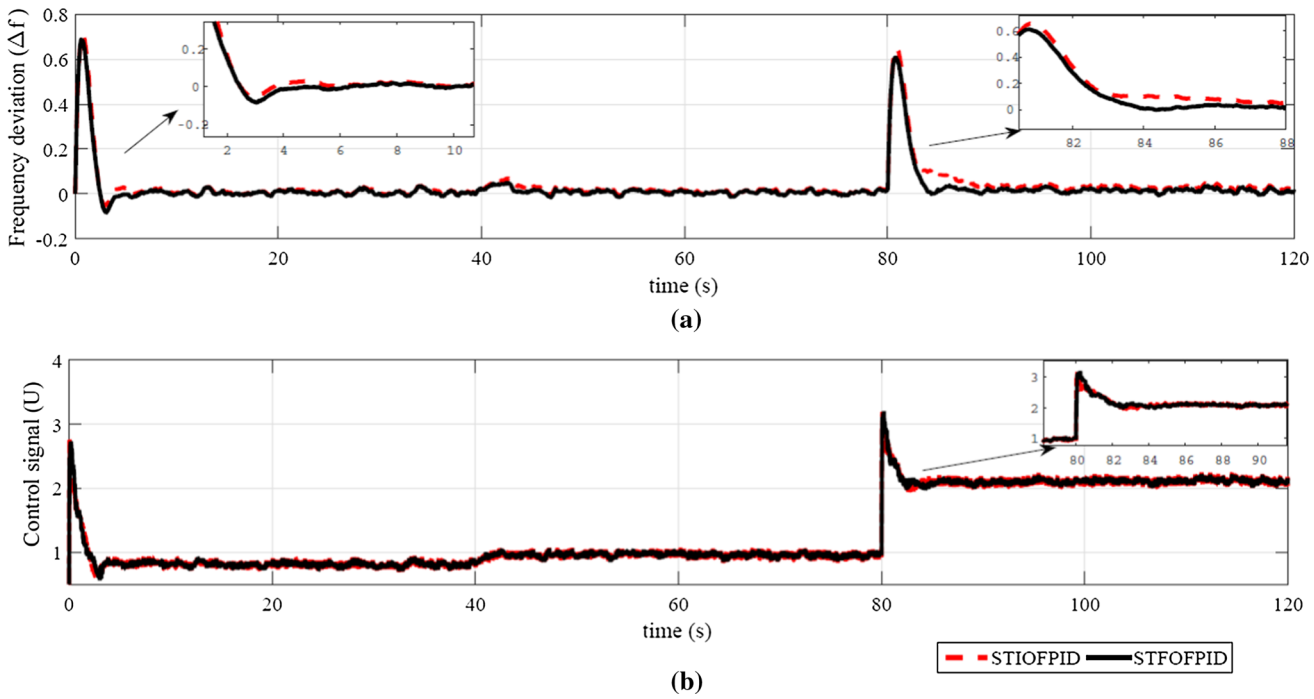

Fig. 8 Frequency deviation and control signal variation for both STIOFPID and STFOFPID controllers

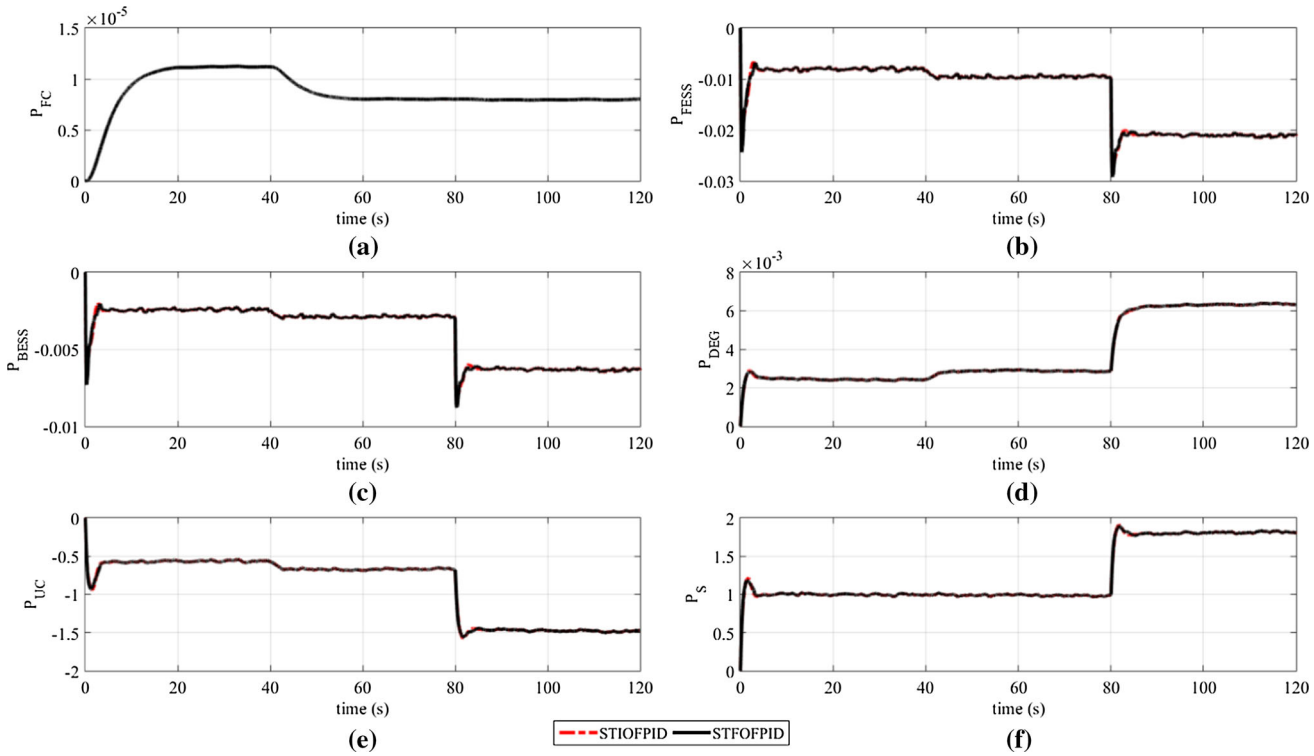

Fig. 9 Power generated by different components of integrated power system: **a** FC, **b** FESS, **c** BESS, **d** DEG, **e** UC and **f** S

5.2 Performance analysis for nonlinear energy storage/production elements in the feedback path

In order to verify the robustness of the controllers used in this paper, the first thing tested is the ability of controllers, viz. STIOFPID and STFOFPID against significant nonlinearities in devices like FESS, BESS, UC and DEG. All these mentioned components are considered to have a rate constraint-type nonlinearity, i.e. saturation. This type of nonlinearity restricts the component by putting limits, to store or release power swiftly, which is an accurate representative of a real-life scenario. This constraint is implemented on different types of first-order energy generation and storage systems with the help of saturation block, having a specified upper and lower cut-off restriction. This nonlinearity is implemented as shown in Fig. 10, just before the integrator in the same path. The various constraints used to implement this nonlinearity are: $|\dot{P}_{\mathrm{FESS}}| < 0.02$, $|\dot{P}_{\mathrm{DEG}}| < 0.001$, $|\dot{P}_{\mathrm{FESS}}| < 1.2$, $|\dot{P}_{\mathrm{BESS}}| < 0.005$. To assess the performances of the controllers under these constraints, the same tuned gains as mentioned in Table 2 were used. Figure 11 shows the deviation of the rate of change of power, for both linear operation and nonlinear rate-constrained operation with optimized controllers wherein it can be seen that the fluctuations are reduced for the case of nonlinearity specially at the transient points at 40 s and 80 s, respectively. Figure 12 shows the effect of nonlinearity on energy-storing/generating components. The objective function values for STIOFPID and STFOFPID controllers are obtained as 4.323 and 4.222, respectively. This clearly shows the superiority in the performance of STFOFPID against its integer-order counterpart, when a saturation-type nonlinearity is introduced in FESS, BESS, UC and DEG.

5.3 Ultracapacitor parameter variation

In this case, controllers' robustness is verified by testing them for the worst case scenario. For the same, UC gain and time constant have been subjected to 30% and 50% increase and decrease, from its nominal values. The reason behind choosing UC for this test is because of the fact that UC has the highest share of power (as observed from Fig. 9e) as compared to other components connected to the feedback path. Therefore, changes in the UC parameters will significantly reflect on the IPS. Table 3 presents ISE, ISDCO and the objective function values for all these four conditions to investigate the robustness. As can be seen from Table 3, the values of ISE and ISDCO, and thus the objective function, J is lower in the case of STFOFPID than in STIOFPID. Therefore, it can be concluded that the fractional-order controller was able to handle parameter variation better and therefore is more robust. By focusing on the improvements in error-based criteria (being the primary objective under controller output limits) and evaluating the relative improvements in maintaining Δf close to zero, a significant difference may be seen between the performances of the STFOFPID and STIOFOFPID, as shown in Table 4 for the case where value of ultracapacitor is changed. It may be inferred from these results that an improvement in the value of ISE and IAE of at least 6.64 and 16.32% and a maximum improvement of 18.47% were achieved. The performance improvement for IAE seems to be larger than ISE value since the variable of interest to be controlled is Δf which is close to zero and hence squaring error value to calculate ISE decreases the value of performance measure, and also the percentage improvement. The same has been demonstrated in Fig. 13, which demonstrates the error and control signal plot for both the controllers. Figure 14 shows the variations in objective functions, with a continuous variation in the UC parameters. Figure 15 presents a column chart comparing the values of J for all the above cases. The UC gain and the time constants were varied from −50 to +50% of the nominal value.

To test the robustness, additional parameter known as the integral of absolute error (IAE) has also been computed. It may be noted that it does not add weight to any of the errors in a system's response and it tends to produce slower response than ISE optimal systems, but usually with less sustained oscillation. The IAE during various tests that have been listed above gives a fair comparison between the two controllers. Under best tuned conditions, IAE of STIOFPID and STFOFPID was recorded as 4.6706 and 3.7752, respectively. As can be observed, STFOFPID performs better in terms of IAE as compared to its integral counterpart.

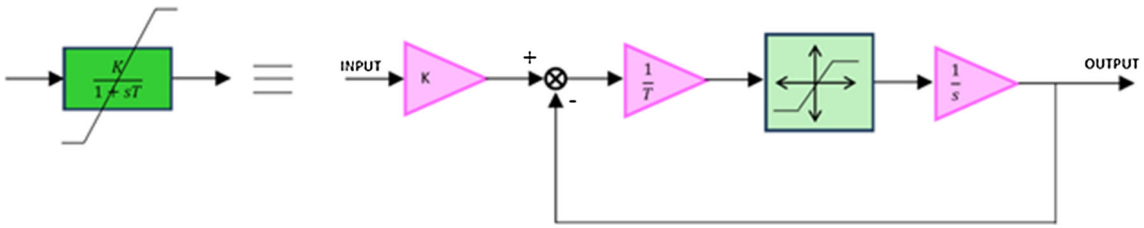

Fig. 10 Typical saturation nonlinearity for a first-order transfer function (rate constraint type)

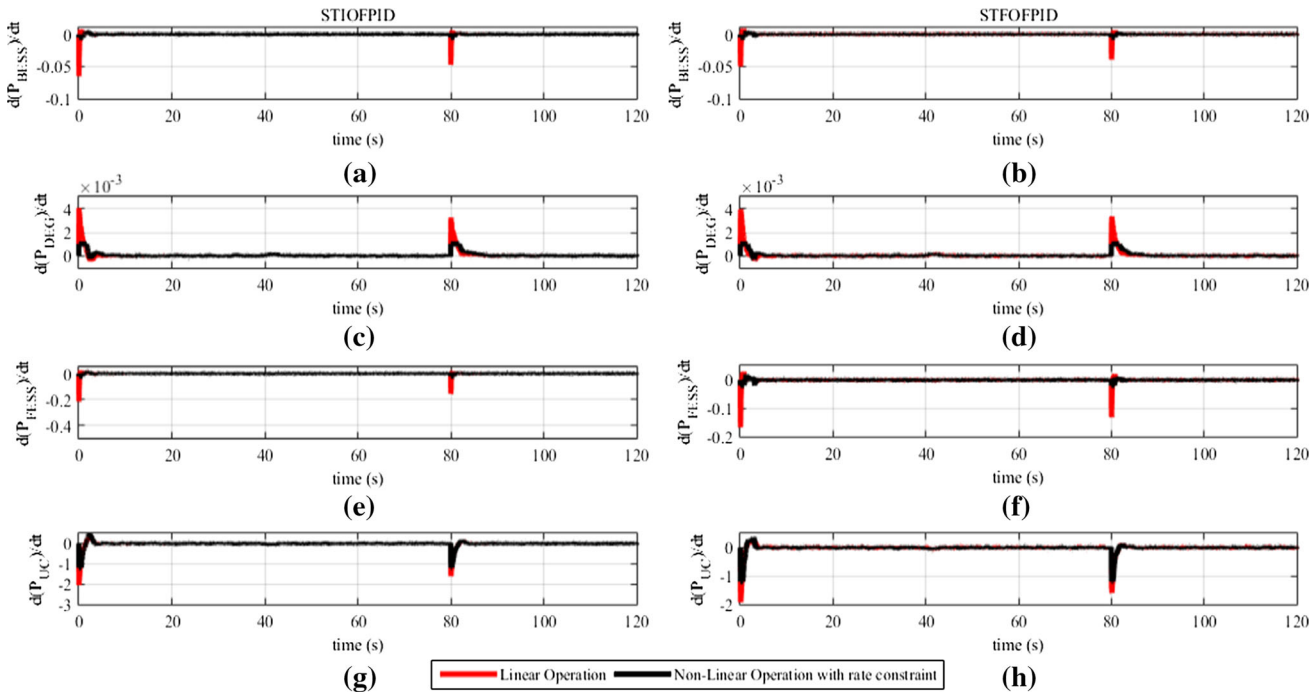

Fig. 11 Effect of nonlinearity on the rates of different components **a**, **c**, **e**, **f** power values of BESS, DEG, FESS and UC, for STIOFPID **b**, **d**, **f**, **h** power values of BESS, DEG, FESS and UC, for STFOFPID

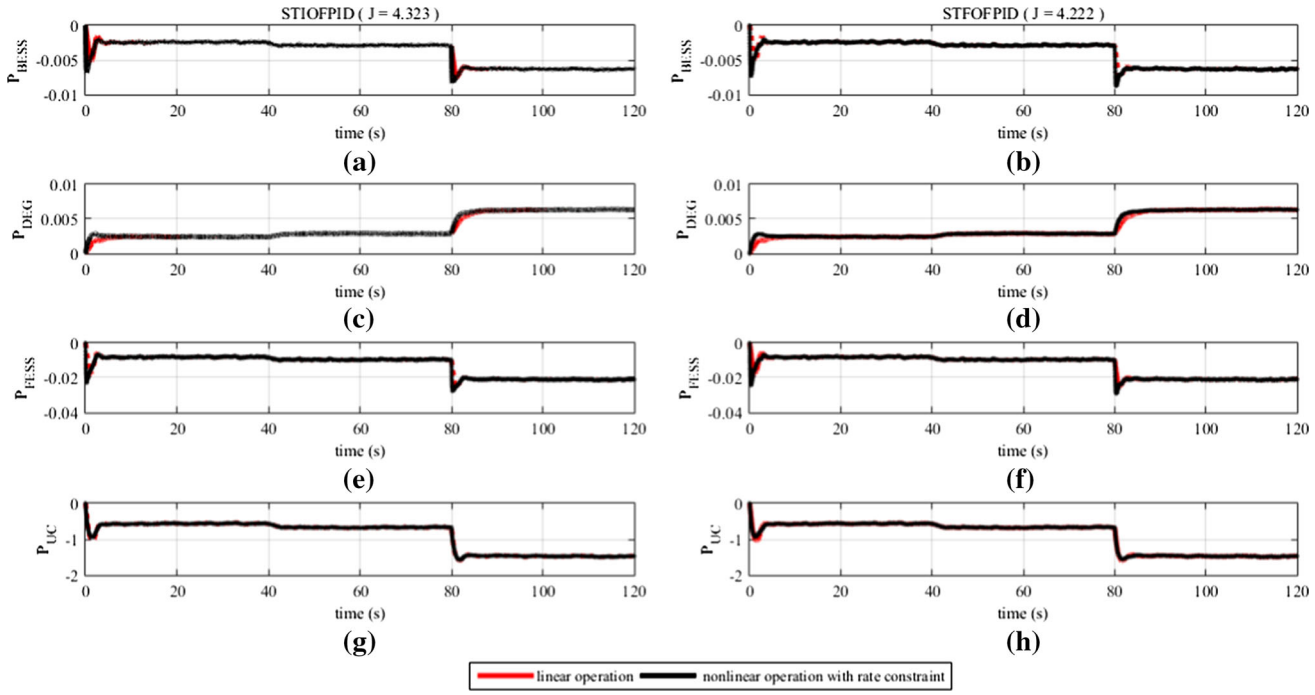

Fig. 12 Effect of nonlinearity on performance of the storage components **a**, **c**, **e**, **f** power values of BESS, DEG, FESS and UC, for STIOFPID **b**, **d**, **f**, **h** power values of BESS, DEG, FESS and UC, for STFOFPID

Table 3 Ultracapacitor parameter variations

Conditions	Performance measure	STIOFPID	STFOFPID
Nominal	ISE	1.22791	1.1391
	ISDCO	2.54768	2.56074
	J	3.7756	3.69985
	IAE	4.67062	3.7850
30% increase	ISE	0.930345	0.868501
	ISDCO	14.4219	14.3599
	J	15.3523	15.2284
	IAE	3.78484	3.10253
50% increase	ISE	0.842923	0.781377
	ISDCO	27.8014	27.7082
	J	28.6443	28.4896
	IAE	3.48937	2.91958
30% decrease	ISE	2.10551	1.94238
	ISDCO	44.8954	45.0817
	J	47.0009	47.0241
	IAE	6.68396	5.42445
50% decrease	ISE	3.88923	3.5066
	ISDCO	224.026	224.66
	J	227.916	228.167
	IAE	9.54979	7.7859

Table 4 Performance improvement for ultracapacitor parameter variations

Conditions	Performance measure	% improvement
Nominal	ISE	07.23
	IAE	18.96
30% increase	ISE	06.64
	IAE	18.02
50% increase	ISE	07.30
	IAE	16.32
30% decrease	ISE	07.74
	IAE	18.84
50% decrease	ISE	09.83
	IAE	18.47

5.4 Removal of different energy storage components

This test is analogous to a real-life scenario. It is always possible that one or more components of the IPS may break down due to the weather, wear and tear, human error or any other reason. Therefore, a controller should also be robust enough to handle the removal of certain energy storage elements. To test the performance of the proposed controller in this case, studies are done by disconnecting/removing different components one at a time and studying the percentage change in performance measures, i.e. ISE/ISDCO from their nominal values. In this study, three cases are considered, viz. separately disconnecting the DEG, FESS and BESS.

To calculate the performance improvement, the following formula has been used. For a particular component x, the performance improvement was computed using (33).

$$\text{Improvement}\% = \frac{(I_{\text{STIOFPID}} - I_{\text{STFOFPID}})}{I_{\text{STIOFPID}}} \times 100\%, \qquad (33)$$

Table 5 presents a performance comparison between the considered controllers for the nominal case and also the cases when an energy storage/generating component was disconnected from the system. Further, Table 6 presents the performance improvement achieved by STFOFPID over STIOPID in terms of ISE for the considered cases. From Table 5, it can be clearly seen that the removal of FESS hugely impacts the whole system and has a higher disruption level on the performance of the controller, followed by BESS and then DEG. Flywheels potentially last for a very long time unlike batteries, which need regular and very expensive replacement perhaps every three or four years. They are extremely efficient and take up less space than batteries so they form a very integral part of the IPS. From Table 5, it can be noted that both the controllers employed here do a decent job of maintaining the severity of the performance deterioration to a minimum. The percentage improvement for this test is shown in Table 6, and it may be inferred that a minimum of 16.41% and maximum of 16.46% improvement is achieved by STFOFPID controller, in case of failure of the considered power source. Figure 16 shows the variation in J, under all four conditions. This proves that the controllers employed will handle the sudden disconnection of different energy storage components without much trouble.

5.5 Performance analysis under varying random noise

Due to the highly stochastic nature of IPS, it becomes necessary to evaluate the performances of the controllers under varying random noise. For this analysis, 100 independent performances in terms of objective function value were recorded for further statistical analysis. A simple statistical analysis tells us about the comparative performance of the controllers employed in IPS. Table 7 presents the statistical analysis of both the controllers. It can be clearly seen that both the average and the standard deviation are less in case of STFOFPID than in STIOFPID, thus again proving its superiority. Figure 17 presents these results in a graphical form. Another statistical analysis was done with a condition when FESS is removed from IPS to

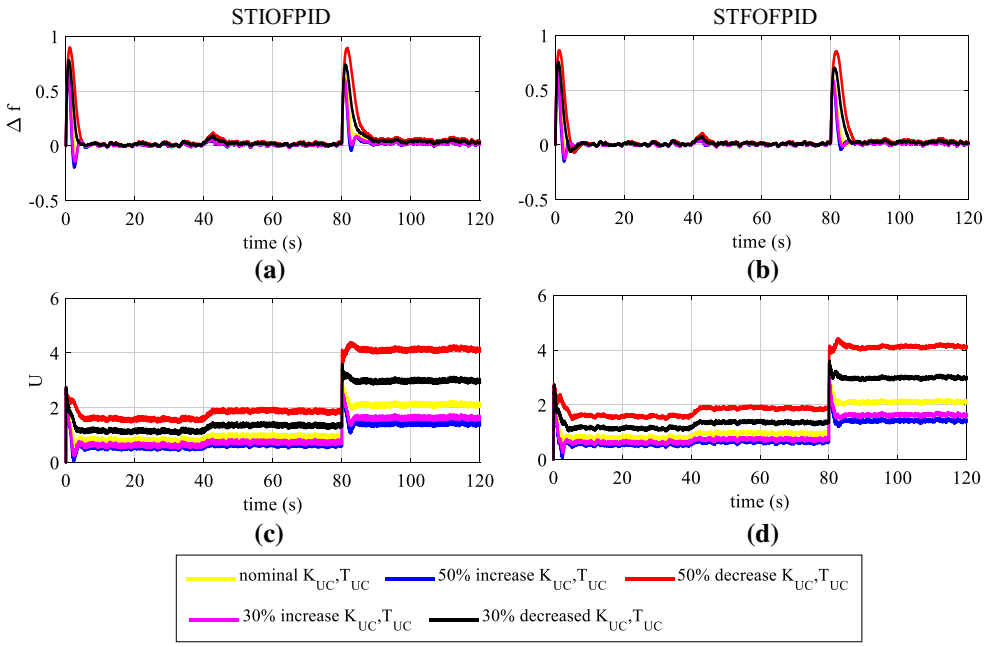

Fig. 13 Control and frequency deviation with varying UC parameters **a**, **b** frequency deviation plot for STIOFPID and STFOFPID. **c**, **d** Control signal plot for STIOFPID and STFOFPID

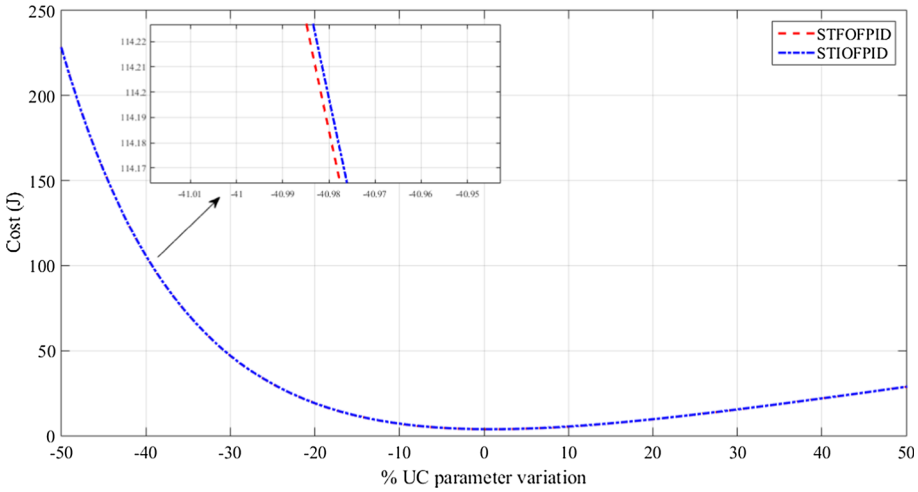

Fig. 14 Variation of objective function value, with percentage increase/decrease in UC parameters

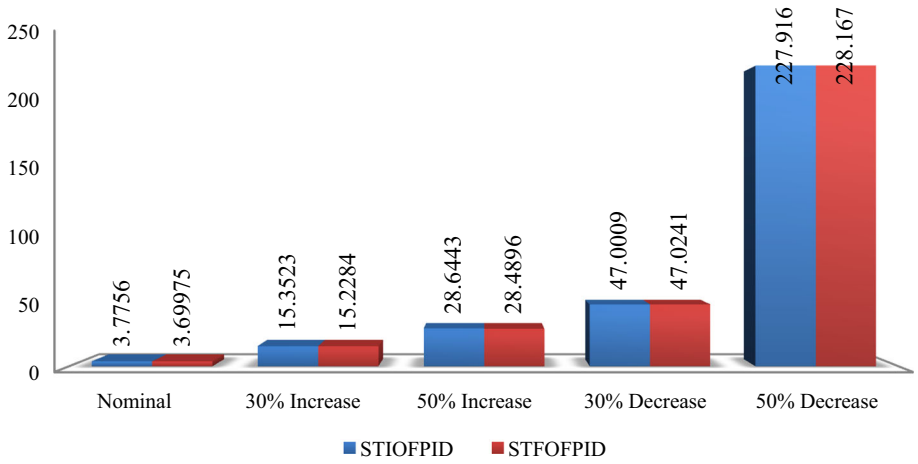

Fig. 15 Variation of J with respect to varying UC parameters at 30%, 50% increase and decrease

Table 5 Performance comparison when disconnecting different components

Component	Performance measure	STIOFPID	STFOFPID
Nominal	ISE	1.22791	1.1391
	ISDCO	2.54768	2.56074
	J	3.7756	3.69985
DEG	ISE	1.23532	1.03195
	ISDCO	2.56692	2.71683
	J	3.80224	3.74878
FESS	ISE	1.27501	1.06568
	ISDCO	2.78611	2.95705
	J	4.06112	4.02277
BESS	ISE	1.24171	1.03787
	ISDCO	2.6074	2.76222
	J	3.8491	3.8001

Table 6 Performance improvement in ISE while disconnecting different components

Component	ISE Values		% improvement
	STIOFPID	STFOFPID	
Nominal	1.22791	1.1391	07.23
DEG	1.23532	1.03195	16.46
FESS	1.27501	1.06568	16.41
BESS	1.24171	1.03787	16.41

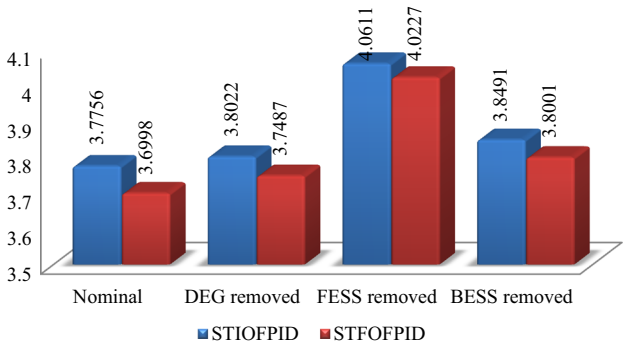

Fig. 16 Variation of J with disconnection of some parameters

Table 7 Statistical analysis under nominal conditions

Controller	Average J (100 iterations)	Standard Deviation
STIOFPID	4.109652	0.265073
STFOFPID	4.048094	0.238039

showcase the robustness of the STFOFPID controller. The quantitative comparison has been shown in Table 8. Again, it was observed that the STFOFPID controller provided better performance in terms of error-based performance criterion as well as aggregate performance criterion. Also,

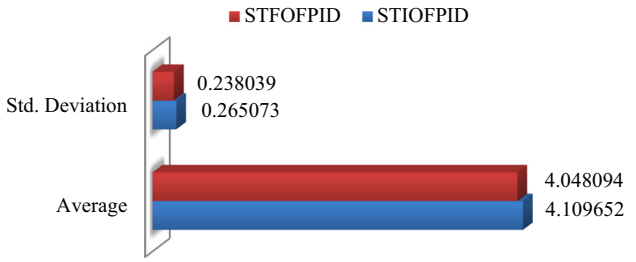

Fig. 17 Graph showing the difference in the average and the standard deviation of the controllers

Table 8 Statistical analysis with FESS removed from IPS

Controller	Average ISE	Average IAE	Average J (100 experiments)	Standard Deviation
STIOFPID	1.42358	5.23243	4.35269	0.27268
STFOFPID	1.21641	4.56377	4.18745	0.23402

the standard deviation of the fractional-order controller is lesser than the integer-order controller, i.e. STIOFPID controller.

6 Conclusions and discussions

In this paper, an attempt has been made to juxtapose self-tuned integer-order fuzzy PID (STIOFPID) controller and self-tuned fractional-order fuzzy PID (STFOFPID) controller applied to efficiently control the integrated power system (IPS). The used IPS employed various generation systems like diesel engine generator (DEG), fuel cell (FC), solar thermal power generation (STPG), wind turbine generator (WTG) and aqua electrolyzer (AE) and energy storage systems such as flywheel energy storage system (FESS), battery energy storage system (BESS) and ultra-capacitor (UC). These self-tuned controllers are Takagi–Sugeno model-based nonlinear adaptive fuzzy controllers whose parameters were optimized by cuckoo search algorithm on the basis of the objective function value defined as the sum of integral of squared error and integral of squared deviation of controller output, for the effective frequency variation control in the predefined load power. Under nominal conditions, it was observed that the STFOFPID controller demonstrated better performance as compared to the STIOFPID controller.

In order to test the robustness of controllers, different case studies were carried out. These studies included, introduction of a rate type saturation nonlinearity in the paths of certain energy storage/generation elements, UC parameters variation and disconnection of certain energy

storage elements from IPS. Additionally, performance analysis was also performed under varying random noise to compare both the controllers. Based on the intensive simulation studies, it was observed that STFOFPID offered better results when FESS, BESS, UC and DEG were subjected to saturation. For UC parameter variations, again STFOFPID offered a superior performance over its integer-order counterpart. Further, certain blocks such as BESS, DEG and FESS were disconnected one by one and performance of both the controllers was evaluated for the predefined objective function, and it was again observed that STFOFPID relatively performed better than STIOFPID. Finally, a simple performance analysis for 100 individual iterations reiterated the superiority of STFOFPID controller over the STIOFPID. Overall, based on the presented investigations STFOFPID controller is concluded to an efficient and robust technique to control the IPS as compared to STIOFPID controller.

Compliance with ethical standards

Conflict of interest The authors certify that they have NO affiliations with or involvement in any organization or entity with any financial interest or non-financial interest in the subject matter or materials discussed in this manuscript.

References

1. Hvelplund F (2006) Renewable energy and the need for local energy markets. Energy 31(13):2293–2302
2. Carrasco JM, Franquelo LG, Bialasiewicz JT, Galván E, PortilloGuisado RC, Prats MM, León JI, Moreno-Alfonso N (2006) Power-electronic systems for the grid integration of renewable energy sources: A survey. IEEE Trans Ind Electron 53(4):1002–1016
3. Morais H, Kadar P, Faria P, Vale ZA, Khodr HM (2010) Optimal scheduling of a renewable micro-grid in an isolated load area using mixed-integer linear programming. Renew Energy 35(1):151–156
4. Katiraei F, Iravani MR, Lehn PW (2005) Micro-grid autonomous operation during and subsequent to islanding process. IEEE Trans Power Deliv 20(1):248–257
5. Khaligh A, Li Z (2010) Battery, ultracapacitor, fuel cell, and hybrid energy storage systems for electric, hybrid electric, fuel cell, and plug-in hybrid electric vehicles: state of the art. IEEE Trans Veh Technol 59(6):2806–2814
6. Li Y, Vilathgamuwa DM, Loh PC (2004) Design, analysis, and real-time testing of a controller for multibus microgrid system. IEEE Trans Power Electron 19(5):1195–1204
7. Illindala M, Venkataramanan U (2002) Control of distributed generation systems to mitigate load and line imbalances. In: Power electronics specialists conference. pesc 02. 2002 IEEE 33rd Annual (vol 4, pp 2013–2018)
8. Ray PK, Mohanty SR, Kishor N (2011) Proportional–integral controller based small-signal analysis of hybrid distributed generation systems. Energy Convers Manag 52(4):1943–1954
9. Rivera DE, Morari M, Skogestad S (1986) Internal model control: PID controller design. Ind Eng Chem Process Des Dev 25(1):252–265
10. Åström KJ, Hägglund T (2006) Advanced PID controllers. 1st edn. ISA-The Instrumentation, Systems and Automation Society, Research Triangle Park, North Carolina, USA
11. Astrom KJ (1995) PID controllers: theory, design and tuning. Instrument society of America, Pittsburgh
12. Ang KH, Chong G, Li Y (2005) PID control system analysis, design, and technology. IEEE Trans Control Syst Technol 13(4):559–576
13. Toscano R (2005) A simple robust PI/PID controller design via numerical optimization approach. J Process Control 15(1):81–88
14. Khan AA, Rapal N (2006) Fuzzy PID controller: design, tuning and comparison with conventional PID controller. In: IEEE international conference on engineering of intelligent systems 2006 (pp 1–6)
15. Kumar V, Nakra BC, Mittal AP (2011) A review on classical and fuzzy pid controllers. Int J Intell Control Syst 16(3):170–181
16. Zadeh LA (1965) Fuzzy sets. Inf Control 8(3):338–353
17. Zadeh LA (1975) The concept of a linguistic variable and its application to approximate reasoning—I. Inf Sci 8(3):199–249
18. Zadeh LA (1975) The concept of a linguistic variable and its application to approximate reasoning—II. Inf Sci 8(4):301–357
19. Zadeh LA (1975) The concept of a linguistic variable and its application to approximate reasoning-III. Inf Sci 9(1):43–80
20. Mamdani EH (1974) Application of fuzzy algorithms for control of simple dynamic plant. Proc IEE (Control Sci) 121(12):1585–1588
21. Mamdani EH, Assilian S (1975) An experiment in linguistic synthesis with a fuzzy logic controller. Int J Man Mach Stud 7(1):1–13
22. Mamdani EH (1976) Advances in the linguistic synthesis of fuzzy controllers. Int J Man Mach Stud 8(6):669–678
23. Mamdani EH, Assilian S (1999) An experiment in linguistic synthesis with a fuzzy logic controller. Int J Hum Comput Stud 51(2):135–147
24. Holmblad LP, Ostergaard JJ (1982) Control of a cement kiln by fuzzy logic. In: Gupta MM, Sanchez E (eds) Fuzzy information and decision processes. Elsevier, North-Holland, pp 389–399
25. Kickert WJ, Mamdani EH (1978) Analysis of a fuzzy logic controller. Fuzzy Sets Syst 1(1):29–44
26. Lee CC (1990) Fuzzy logic in control systems: fuzzy logic controller. I. IEEE Trans Syst Man Cybern 20(2):404–418
27. Lee CC (1990) Fuzzy logic in control systems: fuzzy logic controller. II. IEEE Trans Syst Man Cybern 20(2):419–435
28. Maeda M, Murakami S (1988) A design for a fuzzy logic controller. Inf Sci 45(2):315–330
29. Maeda M, Murakami S (1992) A self-tuning fuzzy controller. Fuzzy Sets Syst 51(1):29–40
30. Wang LX (1993) Stable adaptive fuzzy control of nonlinear systems. IEEE Trans Fuzzy Syst 1(2):146–155
31. Choi BJ, Kwak SW, Kim BK (1999) Design of a single-input fuzzy logic controller and its properties. Fuzzy Sets Syst 106(3):299–308
32. Zhu Q, Azar AT (eds) (2015) Complex system modelling and control through intelligent soft computations. Springer, Germany
33. Boulkroune A, Hamel S, Azar AT, Vaidyanathan S (2016) Fuzzy control-based function synchronization of unknown chaotic systems with dead-zone input. In: Vaidyanathan S, Azar AT (eds) Advances in chaos theory and intelligent control. Springer International Publishing, New York, pp 699–718
34. Meghni B, Dib D, Azar AT (2017) A second-order sliding mode and fuzzy logic control to optimal energy management in wind turbine with battery storage. Neural Comput Appl 28(6):1417–1434

35. Boulkroune A, Bouzeriba A, Bouden T, Azar AT (2016) Fuzzy adaptive synchronization of uncertain fractional-order chaotic systems. In: Vaidyanathan S, Azar AT (eds) Advances in chaos theory and intelligent control. Springer International Publishing, New York, pp 681–697
36. Azar AT, Vaidyanathan S, DeMarco A (eds) (2015) Handbook of research on advanced intelligent control engineering and automation. Engineering Science Reference
37. Azar AT, Vaidyanathan S (eds) (2014) Computational intelligence applications in modeling and control, vol 575. Springer, New York
38. Sugeno M (1985) An introductory survey of fuzzy control. Inf Sci 36(1):59–83
39. Sharma R, Rana KPS, Kumar V (2014) Performance analysis of fractional order fuzzy PID controllers applied to a robotic manipulator. Expert Syst Appl 41(9):4274–4289
40. Kumar V, Rana KPS, Kumar J, Mishra P, Nair SS (2017) A robust fractional order fuzzy P + fuzzy I + fuzzy D controller for nonlinear and uncertain system. Int J Autom Comput 14(4):474–488
41. Kumar V, Rana KPS, Mishra P (2016) Robust speed control of hybrid electric vehicle using fractional order fuzzy PD and PI controllers in cascade control loop. J Franklin Inst 353(8):1713–1741
42. Ghoudelbourk S, Dib D, Omeiri A, Azar AT (2016) MPPT control in wind energy conversion systems and the application of fractional control (PIα) in pitch wind turbine. Int J Model Identif Control 26(2):140–151
43. Azar AT, Vaidyanathan S, Ouannas A (eds) (2017) Fractional order control and synchronization of chaotic systems, vol 688. Springer, New York
44. Das DC, Roy AK, Sinha N (2012) GA based frequency controller for solar thermal–diesel–wind hybrid energy generation/energy storage system. Int J Electr Power Energy Syst 43(1):262–279
45. Lee DJ, Wang L (2008) Small-signal stability analysis of an autonomous hybrid renewable energy power generation/energy storage system part I: time-domain simulations. IEEE Trans Energy Convers 23(1):311–320
46. Raviraj VSC, Sen PC (1997) Comparative study of proportional-integral, sliding mode, and fuzzy logic controllers for power converters. IEEE Trans Ind Appl 33(2):518–524
47. Aslam F, Kaur G (2011) Comparative analysis of conventional, P, PI, PID and fuzzy logic controllers for the efficient control of concentration in CSTR. Int J Comput Appl 17(6):12–16
48. Mishra P, Kumar V, Rana KPS (2015) A fractional order fuzzy PID controller for binary distillation column control. Expert Syst Appl 42(22):8533–8549
49. Ding Y, Ying H, Shao S (1999) Structure and stability analysis of a Takagi–Sugeno fuzzy PI controller with application to tissue hyperthermia therapy. Soft Comput 2(4):183–190
50. Yang XS, Deb S (2010) Engineering optimisation by cuckoo search. Int J Math Model Numer Optim 1(4):330–343
51. Yang XS, Deb S (2014) Cuckoo search: recent advances and applications. Neural Comput Appl 24(1):169–174
52. Mishra P, Kumar V, Rana KPS, Nair SS, Kumar J (2016) Cuckoo search implementation in LabVIEW. In: International conference on computational techniques in information and communication technologies (ICCTICT), pp 331–336
53. Yang XS, Deb S (2009) Cuckoo search via Lévy flights. In: World Congress on Nature & Biologically Inspired Computing, NaBIC, pp 210–214
54. Rajabioun R (2011) Cuckoo optimization algorithm. Appl Soft Comput 11(8):5508–5518
55. Civicioglu P, Besdok E (2013) A conceptual comparison of the Cuckoo-search, particle swarm optimization, differential evolution and artificial bee colony algorithms. Artif Intell Rev 39(4):315–346